

1                   **Membrane fabricated via a facile non-solvent induced**  
2                   **microstructure re-arrangement with superior CO<sub>2</sub> separation**  
3                   **performances**

4                   Jing Wei<sup>1,2,3,4</sup>, Yulei Ma<sup>1,2,3,4</sup>, Zikang Qin<sup>1,2,3,4</sup>, Ziheng Jin<sup>1,2,3,4</sup>, Yao Jin<sup>5</sup>, Lin  
5                   Yang<sup>1,2,3,4\*</sup>, Lu Yao<sup>1,2,3,4</sup>, Wenju Jiang<sup>1,2,3,4</sup>, Yi Deng<sup>6,7</sup>, Ya Huang<sup>6</sup>, Hongyong  
6                   Zhao<sup>8,9</sup>, Jie Dong<sup>8,9</sup>, Liyuan Deng<sup>10</sup>, Zhongde Dai<sup>1,2,3,4\*</sup>

7                   <sup>1</sup>College of Architecture and Environment, Sichuan University, Chengdu 610065, China

8                   <sup>2</sup>National Engineering Research Centre for Flue Gas Desulfurization, Chengdu 610065, China

9                   <sup>3</sup>Carbon Neutral Technology Innovation Center of Sichuan, Chengdu 610065, China

10                  <sup>4</sup>School of Carbon Neutrality Future Technology, Sichuan University, Chengdu 610065, China

11                  <sup>5</sup>College of Biomass Science and Engineering, Sichuan University, Chengdu 610065, China

12                  <sup>6</sup>DongFang Boiler Co.,Ltd., Chengdu 611731, China

13                  <sup>7</sup>Clean Combustion and Flue Gas Purification Key Laboratory of Sichuan Provincial, Chengdu 611731,  
14                  China

15                  <sup>8</sup>State Key Laboratory of Separation Membranes and Membrane Processes/National Center for  
16                  International Joint Research on Separation Membranes, Tiangong University, Tianjin 300387, China

17                  <sup>9</sup>School of Chemical Engineering and Technology, Tiangong University, Tianjin 300387, China

18                  <sup>10</sup>Department of chemical engineering, Norwegian University of Science and Technology, Trondheim,  
19                  7491, Norway

20                  \*Corresponding Author:

21                  Lin Yang: [evanlinyang@sina.com](mailto:evanlinyang@sina.com)

22                  Zhongde Dai: [zhongde.dai@scu.edu.cn](mailto:zhongde.dai@scu.edu.cn),

23  
24                  **Key Words:** CO<sub>2</sub> separation, Block copolymer, Microstructure re-arrangement, Pebax  
25                  membrane

26  
27                  **Abstract:**

28                  CO<sub>2</sub> capture and storage (CCS) is taken as an immediate solution to mitigate the  
29                  impact of increasing atmospheric CO<sub>2</sub> on global climate change, and CO<sub>2</sub> separation  
30                  using high-performance membranes is considered a green and energy-efficient  
31                  technology in CCS. In this study, we developed a novel non-solvent induced  
32                  microstructure re-arrangement method to improve CO<sub>2</sub> separation properties of block

33 copolymer-based membranes, e.g., Pebax 2533. Experiments demonstrate that  
34 microstructure re-arrangement in deionized (DI) water significantly enhances gas  
35 separation performances of Pebax 2533 and reveal that the CO<sub>2</sub>/N<sub>2</sub> selectivity of the  
36 treated membranes remains stable with the CO<sub>2</sub> permeability increased by three folds  
37 to 782.3 Barrers. These findings suggest that microstructure re-arrangement can be a  
38 practical method to improve CO<sub>2</sub> separation performance of block copolymer-based  
39 membrane materials, enabling a broad application in developing gas separation  
40 membranes.

41

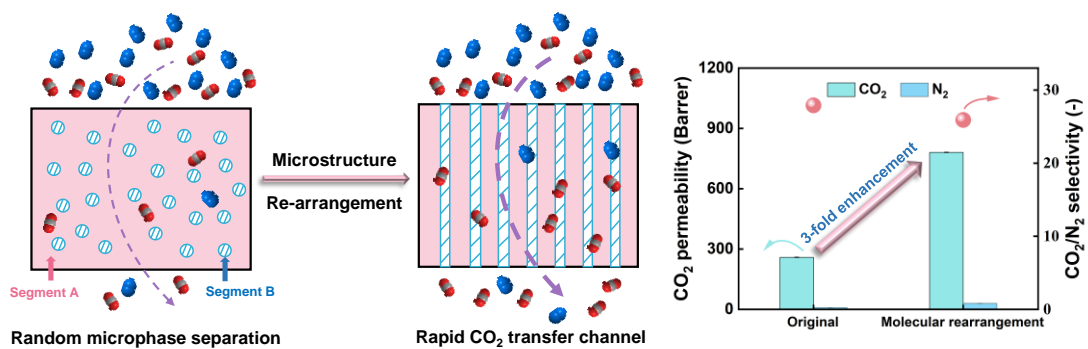
42 **Highlights:**

- 43 \* Non-solvent induced microstructure re-arrangement of block copolymers is studied;
- 44 \* Microstructure re-arranged Pebax 2533 membranes show greatly improved CO<sub>2</sub>  
45 separation performance;
- 46 \* Simple treatment of Pebax 2533 membrane by DI water enables an increase of CO<sub>2</sub>  
47 permeability by three folds;
- 48 \* The effects of re-arrangement conditions were studied to optimize the membrane  
49 microstructure.
- 50 \* The rearranged membrane demonstrated good long-term stability after 300 days  
51 storage

52 .

53

54 **Graphic abstract:**



55

CO<sub>2</sub> N<sub>2</sub> ↓ Gas transportation path

56

## 57 **1. Introduction**

58 It is well-known that carbon dioxide (CO<sub>2</sub>) emissions are the main cause of global  
59 climate anomalies [1]. Therefore, to alleviate the global climate change caused by  
60 excessive CO<sub>2</sub> emissions, the development of advanced CO<sub>2</sub> capture technology has  
61 become the focus of scientists [2, 3]. CO<sub>2</sub> capture and storage (CCS) is widely accepted  
62 as an effective, immediate solution to mitigate CO<sub>2</sub> emission while keeping the usage  
63 of fossil fuels [4]. Among the various CO<sub>2</sub> capture technologies (e.g., absorption,  
64 adsorption, membrane separation, and chemical looping), membrane separation is  
65 considered an emerging technology with enormous potential to improve its process  
66 efficiencies [5], with the advantages of small footprint, energy saving, and linear scaling  
67 up [6]. Up to now, numerous types of membrane materials have been developed for  
68 CO<sub>2</sub> capture, including polymeric membranes [7], mixed matrix membranes(MMMs)  
69 [8], and inorganic membranes (e.g., carbon molecule sieve (CMS) membranes [9],  
70 metal organic framework (MOF) membranes [10] and 2D materials based membranes  
71 [11]). The polymeric membrane is currently the most intensively studied and used CO<sub>2</sub>  
72 separation membrane materials due to its excellent processability, relatively low price,  
73 and moderate CO<sub>2</sub> separation performances [12]. However, most polymeric membranes  
74 suffer from the permeability-selectivity trade-off and the CO<sub>2</sub> separation performances  
75 below the famous Robeson upper bound [13]. There is an urgent need to develop  
76 membrane materials with high CO<sub>2</sub> separation performance and good long-term  
77 stability to further enhance the competitiveness of membrane-based CO<sub>2</sub> separation  
78 processes.

79 Block copolymer is a special type of polymer consisting of a series of alternating  
80 flexible and crystalline hard segments that integrate the excellent properties of different  
81 segments [14]. In the case of block copolymer based membranes, the soft chain segment  
82 is the permeable phase of gas, while the hard chains provide mechanical stability to the  
83 material [15]. The combination of the two chain segments can effectively balance the

84 gas separation performance and mechanical properties and has a wide range of  
85 applications in the field of gas separation and water separation [16, 17]. On the other  
86 hand, due to the incompatibility of each chain segment, the block copolymer will  
87 undergo microphase separation during membrane preparation, forming different  
88 microscopic configurations, which, in turn, produce different transport characteristics  
89 [18].

90 In our previous work, attempts have been made to add ionic liquid (IL) 1-butyl-3-  
91 methylimidazolium tetrafluoroborate ([Bmim][BF<sub>4</sub>]) into the sulfonated pentablock  
92 copolymer Nexar (commercialized as Nexar<sup>®</sup>) to prepare a series of hybrid membranes  
93 for CO<sub>2</sub>/N<sub>2</sub> separation [19]. Small-angle X-ray scattering (SAXS) results clearly show  
94 that the microstructure of the hybrid membranes has changed with the presence of IL,  
95 and the CO<sub>2</sub> separation performances thus changed accordingly. In another study, ILs  
96 and polyethylene glycols (PEGs) were added into Nafion<sup>®</sup> as additives to make hybrid  
97 membranes [20], where the ILs and PEGs not only worked as plasticizers of the  
98 polymeric chains but also tuned the microstructure of the Nafion<sup>®</sup> matrix, with  
99 significant changes of the morphology (observed by transmission electron microscope  
100 (TEM) and SAXS). In addition, the CO<sub>2</sub> permeation performances were enhanced for  
101 over 2 orders of magnitudes.

102 On the other hand, as typical block copolymers, poly (ethylene oxide) (PEO)-based  
103 membranes have been widely used in CO<sub>2</sub> separations [21, 22]. Among these polymers,  
104 Pebax is a representative commercial polyether-polyamide block copolymer  
105 thermoplastic elastomer, with flexible PEO segment and rigid polyamide (PA) blocks  
106 [23]. Due to its good mechanical properties, processing possibilities, and moderate CO<sub>2</sub>  
107 separation performances, Pebax has been intensively studied for different CO<sub>2</sub>  
108 separation applications. Researchers found that using different solvents to prepare  
109 Pebax membranes will lead to significantly different CO<sub>2</sub> separation performances [24,  
110 25], but the detailed characterization and in-depth analysis of the microstructure are  
111 missing. In addition, reports about employing proper solvents-non solvents

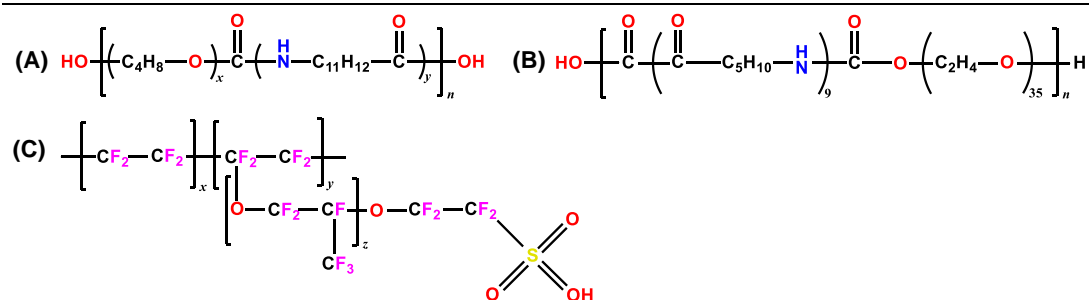
112 combination to optimize the microstructure and improve the membranes separation  
113 performances were intensively studied for liquid separation [26-28], but it can be rarely  
114 seen in gas separation applications.

115 Therefore, in this paper, we propose a facile environmentally friendly method to realize  
116 the microstructure re-arrangement of Pebax 2533 membranes. By using a proper  
117 combination of solvents and non-solvents, the microstructure of the block copolymer-  
118 based membranes can be fine-tuned, and random microstructure is re-constructed to be  
119 more organized, which promotes the formation of high-speed CO<sub>2</sub> transmission  
120 channels and thus improves the membranes' CO<sub>2</sub> separation efficiency. The effects of  
121 different microstructure re-arrangement conditions, e.g., non-solvent type, soaking  
122 duration, and temperature, on the morphology and separation performance of Pebax  
123 membranes were systematically investigated. The gas permeation properties of the  
124 obtained membranes were also tested under different conditions.

## 125 **2. Experimental**

### 126 **2.1 Materials**

127 Commercial Pebax 2533 and Pebax 1657 were ordered from Arkema (France).  
128 Alcohol-based Nafion D520 solution was obtained from Ion Power (Munich, Germany).  
129 Reagent-grade ethanol was purchased from Jinshan Chemical Test Co., Ltd. (Chengdu,  
130 China) and used without further purification. DI water was prepared using a laboratory  
131 water purification system (TE-S20). The CO<sub>2</sub> and N<sub>2</sub> gases used in the experiment were  
132 purchased from Chengdu Xuyuan Chemical Co., Ltd (Chengdu, China), and were used  
133 directly upon receipt. The purity of the single-component gas was 99.999%.



134

135

**Scheme 1.** Molecular structure of Pebax 2533 (A), Pebax 1657 (B), and Nafion D520 (C).

136

## 2.2 Membrane fabrication

137

The membranes were prepared by solution casting, as shown in Scheme 2. A certain amount of Pebax 2533 polymer was weighed into a single-mouth flask, and ethanol was added to obtain an 8 wt.% polymer membrane solution by reflux stirring at 80 °C for 8 h. The solution was then poured into a Teflon petri dish, and the solvent was volatilized for 24 h at room temperature (RT). The membrane was then removed from the casting petri dish and placed in a vacuum oven, where it was dried at 50 °C for 24 h to remove residual solvents and adsorbed impurity gas on the membrane.

143

144

An appropriate amount of Pebax 1657 was added to 70/30 w/w% ethanol/water solution and stirred at 80 °C for 30 min to ensure the Pebax was completely dissolved, and 1.5 wt.% Pebax solution was obtained. The solution was then poured into a Teflon petri dish, and the solvent was volatilized for 24 h at RT. The membrane was then removed from the casting petri dish and placed in a vacuum oven, where it was dried at 50 °C for 24 h to remove residual solvents and adsorbed impurity gas on the membrane.

149

150

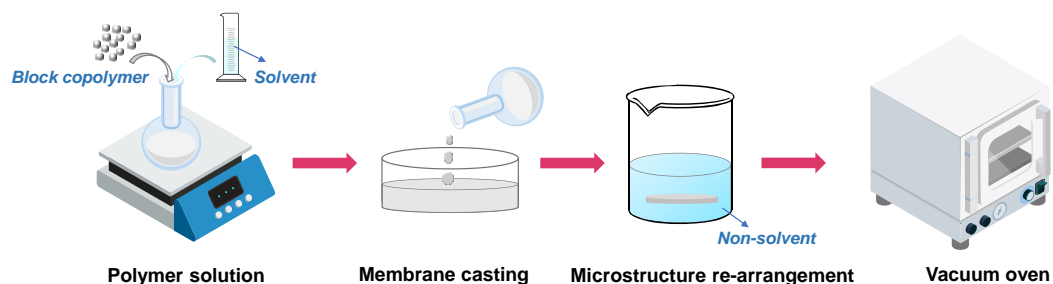
Nafion dispersion was stirred magnetically in a round-bottomed flask for at least 30 minutes. It is then poured into a glass petri dish. To keep the membranes uniform and uncracked, it needs to be heated at 80 °C for 100-120 minutes, while another petri dish is covered with the first one to reduce the evaporation rate of the solvent. After the solution was evaporated, the resulting membrane was dried at 60 °C under vacuum for 6 hours before it was used for subsequent tests.

155

156

For non-solvent induced microstructure re-arrangement, the membranes were

157 immersed in corresponding non-solvent for 24 h and then dried under vacuum at 35 °C  
158 for 24 h before being used for subsequent analysis. The membrane thicknesses were  
159 measured using a Digimatic micrometer (SanLiang, China), and the average of at least  
160 10 measurements over the entire permeating area was recorded.



161

162

**Scheme. 2.** Microstructure re-arrangement membranes fabrication.

### 163 2.3 Membrane characterization

164 Thermogravimetric analysis (TGA) was characterized using a synchronous thermal  
165 analyzer (NETZSCH, STA 449, Germany) with a temperature range of 30-800 °C and  
166 a heating rate of 10 °C min<sup>-1</sup>. To prevent premature degradation, high purity N<sub>2</sub> gas  
167 (99.999%) was used as scanning and protective gas at a flow rate of 60 mL min<sup>-1</sup>. The  
168 differential scanning calorimeter (DSC) (NETZSCH, 204 F1, Germany) was utilized to  
169 determine the basic thermal properties and analyze the glass transition temperature ( $T_g$ )  
170 of different microstructure re-arrangement membranes. The testing procedure consisted  
171 of three steps: first, the membrane was brought up to 150 °C in a high purity N<sub>2</sub>  
172 atmosphere (99.999%) to remove moisture and other impurities, then the sample was  
173 cooled to -150 °C and then again raised to 150 °C at a heating/cooling rate of 10 °C min<sup>-1</sup>.  
174 The second heating ramp was used to analyze the glass transition temperature of the  
175 membrane. Fourier-transform infrared (FTIR) spectroscopy (PerkinElmer, Frontier,  
176 USA) was used to qualitatively analyze the chemical bonds of the membranes, with a  
177 wavelength range of 4000-650 cm<sup>-1</sup>. TEM (FEI, Tecnai G2 F20, USA) was used to  
178 examine the morphology of the membrane. Membrane samples were stained with a  
179 saturated lead acetate aqueous solution and then embedded in epoxy resin for slicing.



180 The chemical composition of the membranes was analyzed by X-ray photoelectron  
181 spectroscopy (XPS) (KRATOS, XSAM 800, UK). The nanostructures of Pebax  
182 membranes were also characterized by SAXS (Nanostar U SAXS, Bruker, Germany).  
183 The sample was exposed to a 14 keV beam (wavelength,  $\lambda=0.154$  nm), and the distance  
184 between the sample and detector was 2 m with a spot size of 0.5 x 0.5 mm. Azimuth  
185 integration of the obtained two-dimensional scattering diagram provided a one-  
186 dimensional intensity distribution of the scattering vector  $q=(4\pi/\lambda) \sin\theta$ , where  $\lambda$  is the  
187 X-ray wavelength and  $\theta$  is the half angle of scattering. The microstructure of the  
188 samples was detected using the X-ray diffractometer (XRD) (Rigaku Ultima IV) with  
189 Cu target wide-angle diffraction. The scanning range was 5~75 °, the scanning rate was  
190 10 ° min<sup>-1</sup>, and the step size was 0.02 °.

191 The liquid water uptake test was performed at RT and atmospheric pressure. The  
192 samples were immersed in DI water for 24 hours. The liquid water uptake was  
193 calculated as follows

$$194 \quad \Omega_{H_2O} = \frac{W_{\infty} - W_D}{W_D} \times 100 \quad (1)$$

195 where  $W_{\infty}$  and  $W_D$  represent the weight of dry and water-saturated membranes,  
196 respectively. According to the average value of the two samples, the experimental error  
197 is less than 5%.

198 Single gas permeability was tested by constant-volume variable-pressure method [29].

199 The gas permeability ( $P$ ) is calculated based on equation (2):

$$200 \quad P = \frac{V_d}{RTA} \times \frac{l}{(p_u - p_d)} \times \left[ \left( \frac{dp}{dt} \right)_{t \rightarrow \infty} - \left( \frac{dp}{dt} \right)_{leak} \right] \quad (2)$$

201 where  $V_d$  is the permeation volume,  $R$  is the universal gas constant,  $T$  is the test  
202 temperature,  $A$  refers to the effective permeation area,  $l$  is the thickness of the  
203 membrane, and  $p_u - p_d$  is the pressure difference across the membrane,  $\left( \frac{dp}{dt} \right)_{t \rightarrow \infty}$  is the  
204 pressure gradient on the downstream side at a steady state, while  $\left( \frac{dp}{dt} \right)_{leak}$  is the leakage  
205 rate of the permeation rig.

206 The corresponding gas ideal selectivity ( $\alpha$ ) is expressed by the ratio of permeability of

207 different gas components:

$$208 \quad \alpha_{ij} = \frac{P_i}{P_j} \quad (3)$$

209 where  $P_i$  and  $P_j$  correspond to the permeability of two different gaseous species  $i$  and  $j$ .  
210 and the gas permeability unit used here is the Barrer. 1 Barrer= $10^{-10}(\text{cm}^3(\text{STP}) \text{ cm}/(\text{cm}^2$   
211  $\text{ s cmHg})$ . For each membrane, the final result is reported as the average of the three  
212 measurements.

### 213 3. Results and discussion

#### 214 3.1 Miscibility and compatibility study

215 To determine the optimal solvent and non-solvent for Pebax 2533, we used the Hansen  
216 solubility parameter (HSP) to screen common solvents [30]. The HSP method utilizes  
217 the difference in solubility parameters between the material and the solvent to  
218 determine the solubility of the solvent to the material, and it is often used for the  
219 preliminary screening of polymer solvents. Hansen extended the solubility theory to  
220 three dimensions, and HSPs are composed of dispersion force ( $\delta_D$ ), polarity force ( $\delta_P$ ),  
221 and hydrogen bonding force ( $\delta_H$ ).

222 To calculate whether a polymer is compatible with the solvent, we can determine the  
223 solubility parameter difference between the polymer and the solvent using Equation 4:

$$224 \quad \Delta\delta = \sqrt{(\delta_{D,i} - \delta_{D,p})^2 + (\delta_{P,i} - \delta_{P,p})^2 + (\delta_{H,i} - \delta_{H,p})^2} \quad (4)$$

225 In the formula:

226  $\Delta\delta$ —Solubility parameter difference,  $\text{MPa}^{0.5}$ ;

227  $\delta_D$ —Dispersion action solubility parameter,  $\text{MPa}^{0.5}$ ;

228  $\delta_P$ —The solubility parameter of polar action,  $\text{MPa}^{0.5}$ ;

229  $\delta_H$ —Hydrogen bonding solubility parameter,  $\text{MPa}^{0.5}$ ;

230 Subscripts  $i$  and  $p$  denote solvent and polymer, respectively.

231 The three-dimensional solubility parameters of materials can be simulated by Hspip

232 software [31]. HSP solubility parameters of Pebax 2533 and commonly used solvents  
 233 for Pebax 2533 are shown in **Table 1**.

234 **Table 1.** Solubility Parameters of solvents/non-solvents for Pebax 2533

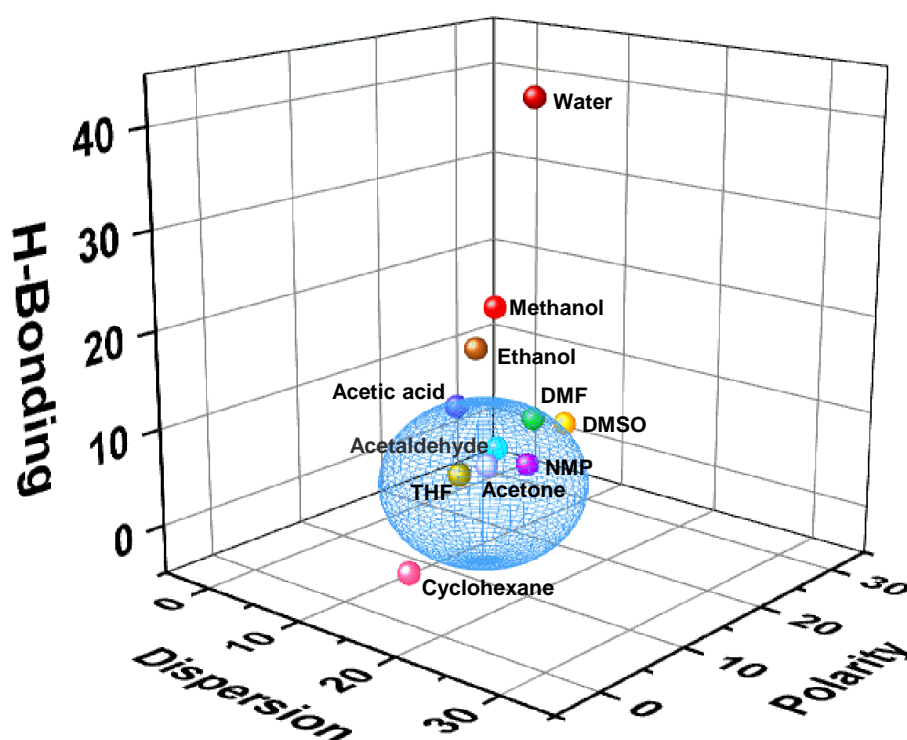
Material	Solubility parameter (MPa <sup>0.5</sup> )				
	$\delta_D^a$	$\delta_P^a$	$\delta_H^a$	$\delta_t^b$	$\Delta\delta$
Pebax 2533	17.6 <sup>c</sup>	7.6 <sup>c</sup>	6.8 <sup>c</sup>	20.3	—
Pebax 1657	18.8	5.4	11.2	22.5	—
Ethanol/water mixture	15.7	11.0	26.3	32.5	—
Ethanol	15.8	8.8	19.4	26.5	12.8
Water	15.5	16	42.3	47.8	36.5
Dimethyl sulfoxide	18.4	16.4	10.2	26.7	9.5
Methanol	15.1	12.3	22.3	29.6	16.4
N, N-Dimethylformamide	17.4	13.7	11.3	24.9	7.6
Tetrahydrofuran	16.8	5.7	8.0	19.4	2.4
N-Methylpyrrolidone	18.0	12.3	7.2	23.0	4.7
Acetic acid	14.5	8.0	13.5	21.4	7.4
Acetaldehyde	14.7	12.5	7.9	20.9	5.8
Acetone	15.5	10.4	7.0	19.9	3.5
Cyclohexane	16.8	0	0.2	16.8	10.1

235 <sup>a</sup> as calculated by HSPiP software.

236 <sup>b</sup>  $\delta_t$ , total cohesion (solubility) parameter:  $\delta_t^2 = \delta_D^2 + \delta_P^2 + \delta_H^2$ .

237 <sup>c</sup> The solubility parameters of Pebax 2533 were calculated from the group constants of  
 238 the polymer structural units [32]

239



240

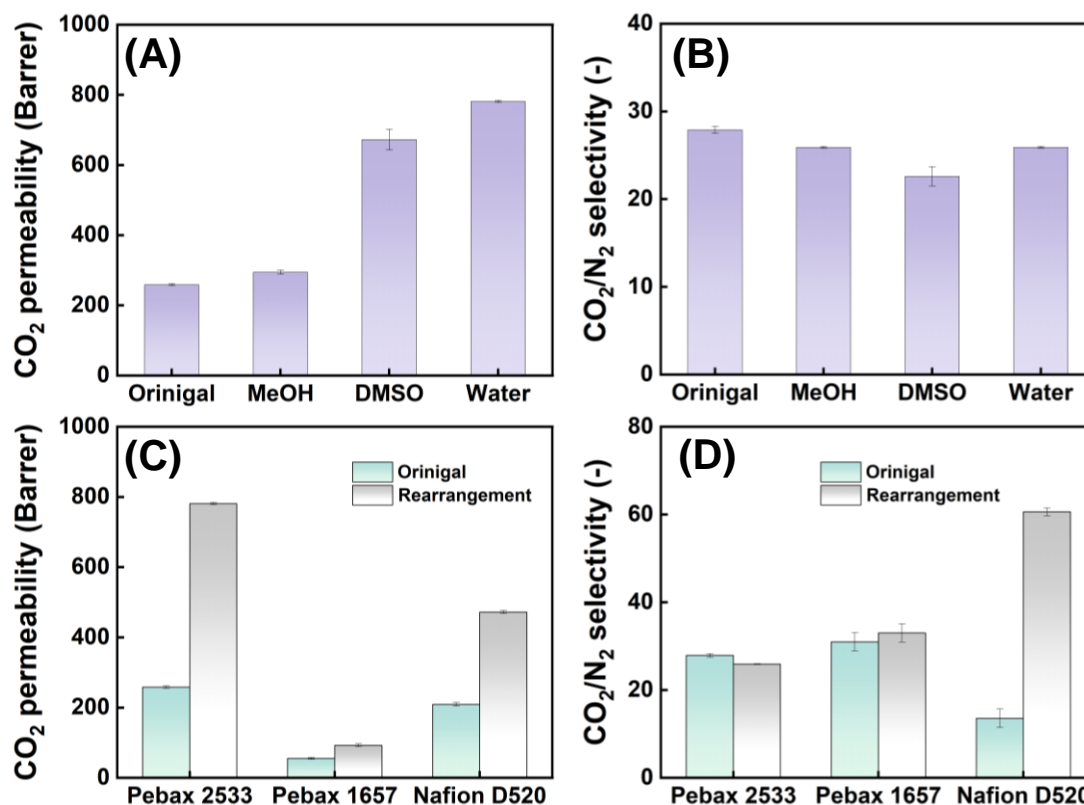
241 **Figure 1.** Plot of solubility parameter for various solvents/non-solvents of Pebax 2533

242 According to the definition of HSPs, a solvent with  $\Delta\delta$  less than 10 is considered a  
243 suitable solvent for a polymer compared to a polymer [24, 33]. **Figure 1** plots the  
244 solubility parameters of each solvent in **Table 1**, with the sphere representing the HSPs  
245 sphere of Pebax 2533 with a radius of 10. The solvent capable of dissolving Pebax 2533  
246 could be located within the sphere area, such as N, N-Dimethylformamide(DMF),  
247 Tetrahydrofuran (THF), and N-Methylpyrrolidone (NMP), which have been applied as  
248 the solvent for Pebax 2533 to prepare membranes for gas separation [34, 35].  
249 Surprisingly, even though ethanol/water are not considered a ‘good’ solvent as  
250 indicated in the HSPs systems, they have been widely used as solvents for Pebax to  
251 prepare gas separation membranes [36-38] due to their low toxicity and good  
252 environmental friendly. A large number of literature have shown that membrane  
253 materials prepared with ethanol and ethanol/water as solvents have higher separation  
254 performance [39-41], possibly due to unexpected micro-structures. Furthermore, the  
255 solubility parameter method can also help us to quickly determine the non-solvent that  
256 can be used for microstructure re-arrangement. In the current study, ethanol/water was

257 used as solvents for Pebax 1657, while the mixture of alcohols was used as solvents for  
258 the Nafion.

### 259 **3.2 Effect of non-solvents**

260 To investigate the effect of non-solvent induced microstructure re-arrangement,  
261 methanol, dimethyl sulfoxide (DMSO), and water was employed as non-solvent, and  
262 the gas permeability of the re-arranged membranes was tested and presented in **Figure**  
263 **2**. Compared to the neat Pebax 2533 membrane, treating the membrane with non-  
264 solvent at RT for 24 hours leads to rather different gas separation performances: the  
265 CO<sub>2</sub> permeability was greatly improved with only a slight reduction in CO<sub>2</sub>/N<sub>2</sub>  
266 selectivity (**Figure 2B**). In addition, among these 3 non-solvents, the water-treated  
267 membrane resulted in the highest CO<sub>2</sub> permeability (782.3 Barrer), which is 3 times the  
268 value of the neat membrane (258.5 Barrer), while the CO<sub>2</sub>/N<sub>2</sub> selectivity was only  
269 slightly reduced from 27.9 to 25.9. Therefore, water was employed as the non-solvent  
270 to induce potential micro-phase separation in Pebax 1657 and Nafion D520 membranes.  
271 The water-induced micro-phase separation resulted in quite different results for Pebax  
272 1657 and Nafion D520 (As shown in **Figure 2C** and **Figure 2D**). It is found that water  
273 has significantly enhanced CO<sub>2</sub> permeability for Pebax 2533 membrane, while it is  
274 more effective in promoting CO<sub>2</sub>/N<sub>2</sub> selectivity for the Nafion D520 membrane. On the  
275 other hand, for Pebax 1657, the water-induced micro-phase separation only leads to  
276 slightly improved CO<sub>2</sub> permeability and CO<sub>2</sub>/N<sub>2</sub> selectivity. In addition, data for Pebax  
277 2533 and Pebax 1657 were obtained using single-gas permeation tests under dry  
278 conditions, while data for Nafion D520 were obtained using mixed-gas tests at 100%  
279 RH.



280

281

**Figure 2.** Effect of non-solvent induced micro-phase separation on gas permeation. CO<sub>2</sub> permeability

282

(A) and CO<sub>2</sub>/N<sub>2</sub> selectivity (B) of Pebax 2533 membranes with different non-solvents; CO<sub>2</sub>

283

permeability (C) and CO<sub>2</sub>/N<sub>2</sub> selectivity (D) of Pebax 2533, Pebax 1657, and Nafion D520. Gas

284

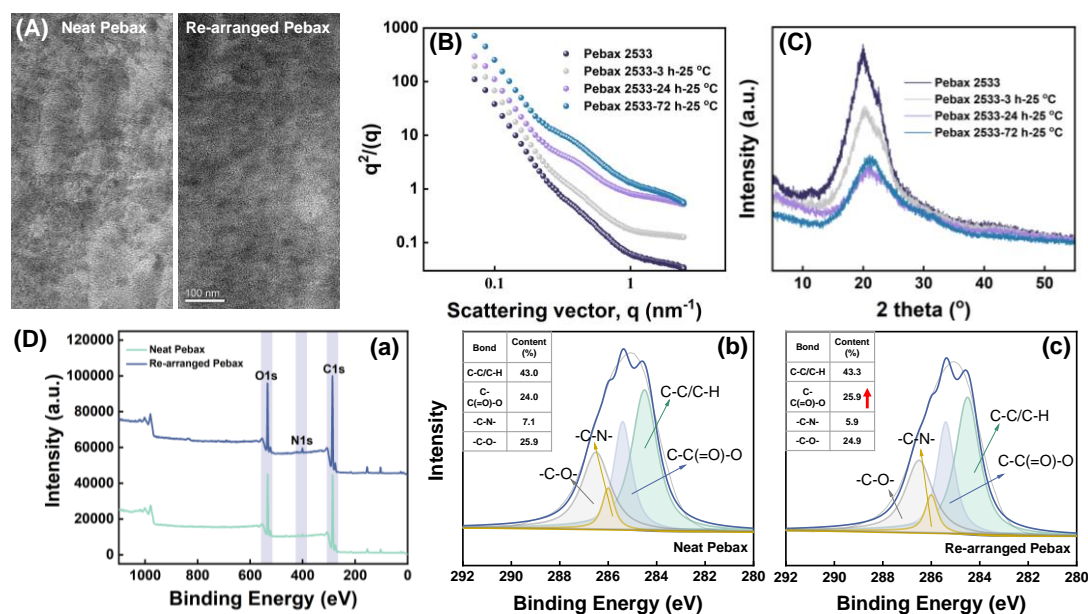
permeation was tested with a feed pressure of 2 bar at 25 °C.

### 285 3.3 Effect of microstructure re-arrange time

286 The Pebax 2533 was further studied by changing the water treatment duration length.

287 The obtained membranes were thoroughly characterized using various technics, and the

288 results are presented in **Figure 3**.



289

290

291

292

293

294

**Figure 3.** Chemical-physical characterization of Pebax 2533 before and after water induced micro-phase separation. TEM image of neat Pebax 2533 and Pebax 2533 soaked in water for 24 hours (A); SAXS (B) and XRD results (C) of Pebax 2533 treated with water for different duration time; XPS spectra of neat Pebax 2533 and Pebax 2533 soaked in water for 24 hours (D) (a: complete survey spectrum, b, c: C 1s spectrum).

295

296

297

298

299

300

301

302

303

304

305

306

307

The mechanism of gas transport within Pebax 2533 is largely determined by the micro-structures before and after re-arrangement. In this study, TEM was used to acquire real-space images of the Pebax 2533 membranes before and after re-arrangement in DI water. Prior to observation, selective staining was performed with saturated lead acetate, so that the PEO region appears electron-opaque (dark), the results of this analysis are presented for comparison in **Figure 3A**. As previously expected in TEM studies of Pebax 2533 [42], the nanostructure is generally irregular, apparently composed of co-continuous hydrophilic (PEO, dark) and hydrophobic (PA, light) features. In contrast, after the microstructure re-arrangement in DI water, Pebax 2533 membrane swelled to form a nanoscale hydrophilic region, resulting in a more homogeneous and connected structure of the hydrophilic network in the membrane, which may lead to rather different CO<sub>2</sub> transport properties. It may also be the result of non-solvent water-induced enhancement of molecular mobility, which contributes to improved spatial

308 separation of highly incompatible hydrophilic and hydrophobic regions.

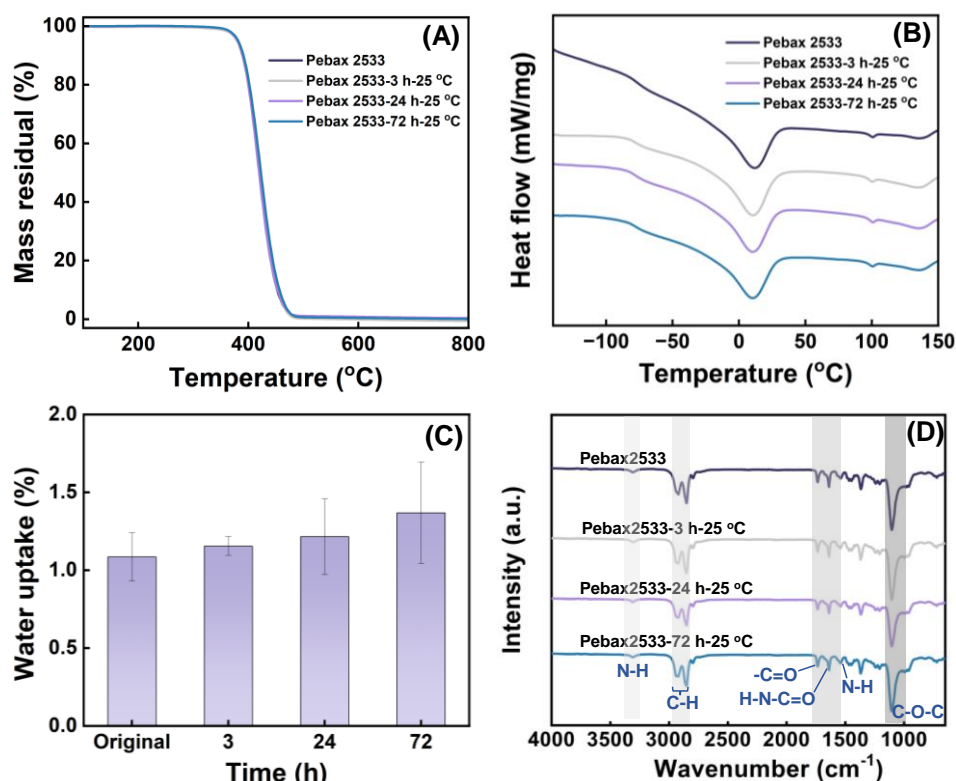
309 The rate of CO<sub>2</sub> transport in Pebax 2533 membranes depends on the size, shape, and  
310 connectivity of the hydrophilic region. TEM provides valuable spatial information  
311 about these morphological features, while SAXS provides a more sensitive way to  
312 distinguish the morphology of the membranes prepared in this study. **Figure 3B**  
313 displays the SAXS profiles collected from membranes derived from Pebax 2533 before  
314 and after re-arrangement (consistent with TEM images provided in **Figure 3A**). The  
315 profile for Pebax 2533 displays a weak peak near the  $q = 0.4 \text{ nm}^{-1}$ , which corresponds  
316 to a characteristic spacing ( $d$ ) of  $\sim 15.7 \text{ nm}$  according to Bragg's law ( $d = 2\pi/q^*$ , where  
317  $q^*$  represents the scattering vector of interest). This characteristic interval is attributed  
318 to the hydrophilic region, consistent with the results of Wilkes et al. [43]. After the  
319 introduction of DI water, with the extension of water treatment time, the peak  
320 broadened significantly and shifted to a lower  $q$ , so the corresponding spacing increases  
321 slightly to  $17.0 \text{ nm}$ , which may contribute positively to the gas permeability.

322 In prior studies [44, 45], TEM combined with SAXS was also used to analyze the  
323 microstructures of polymers before and after re-arrangement. For sulfonated block  
324 copolymer (Nexar), the introduction of ionic liquids (non-solvent) resulted in profound  
325 morphological restructuring, changing from sheet to layered structure. Further  
326 introduction of water vapor leads to swelling of the nanostructures, and this  
327 microstructure transformation significantly improved CO<sub>2</sub> permeability. For Nafion,  
328 another random polymer, the introduction of ionic liquids and water vapor also caused  
329 nanostructures change and consequently improvement in CO<sub>2</sub> separation  
330 performances. XRD is another powerful tool widely used to characterize the Pebax  
331 2533 membranes [36, 47]. In our study, a strong crystallization peak at  $20.4^\circ$  was found  
332 for the neat Pebax 2533 membranes and the membrane after water treatment, which is  
333 attributed to the crystalline region of PA and is consistent with previous reports in the  
334 literature [48] (**Figure 3C**). As expected, soaking the membrane in DI water reduced  
335 the peak intensity in the crystalline region of the Pebax 2533 matrix. Thus, crystallinity



336 decreased with increasing water treatment duration time. This phenomenon is mainly  
337 due to the breaking of hydrogen bonds between the PA segments of Pebax 2533, leading  
338 to a decrease in the binding energy within the microstructure re-arrangement membrane  
339 [49]. As a lower membrane crystallinity degree normally leads to higher CO<sub>2</sub>  
340 permeability, it is expected that the water-treated Pebax membranes will result in high  
341 gas permeability.

342 To further explicate the elemental compositions of the original and rearrangement  
343 membranes, XPS analysis was performed and the results are shown in **Figure 3D (a)**.  
344 As can be seen in **Figure 3D a**, both membranes presented three peaks at 533.2 (O 1s),  
345 400.6 (N 1s), and 286.2 eV (C 1s), the position of the spectral peak remains unchanged  
346 after rearrangement. It can be concluded that the rearrangement by water at 25 °C does  
347 not affect the chemical structure of the Pebax membranes. **Figure. 3D (b) and (c)** show  
348 the C 1s XPS spectra of the original and rearranged membranes. The typical peaks of  
349 C-C/C-H (284.5 eV), C-C(=O)-O (285.4 eV), -C-N- (286.0 eV), and -C-O- (286.5 eV)  
350 were observed for both membranes. It is noted that the content of each bond is almost  
351 unchanged after re-arrangement, suggesting the re-arrangement is mainly a physical  
352 procedure.



353

354 **Figure 4.** Thermal stability (A), DSC (B), water uptake (C), and FTIR spectrum (D) of Pebax 2533

355

membranes treated with water for different duration times.

356

Other than the morphology of the membranes, their thermal properties were also  
357 thoroughly investigated. As expected, the water treatment is mainly a physical  
358 procedure that does not lead to any chemical change in the membrane materials. Thus,  
359 the thermal stability of the Pebax 2533 before and after water treatment was almost the  
360 same (**Figure 4A**); increasing water soaking time leads to no change in the thermal  
361 stability of Pebax 2533 membranes. In addition, the thermal decomposition temperature  
362 of all membrane materials is above 350 °C, indicating that they can meet the separation  
363 requirements under high-temperature conditions [50].

364

On the other hand, DSC test was also carried out for the Pebax 2533 membranes. The  
365 second heating cycle results were analyzed to eliminate surface and internal moisture  
366 and impurities. It is well-known that Pebax 2533 is a partially crystalline block  
367 copolymer consisting of an amorphous PEO phase and a crystalline PA phase [51].

368

Prior to was induced microstructure re-arrangement, Pebax 2533 exhibited two melting

369 point peaks ( $T_m$ ) at 11.36 °C (PEO segment) and 100.76 °C (PA segment), respectively,  
370 indicating the presence of phase separation in the Pebax 2533 membrane, which is  
371 consistent with literature reports [52]. As shown in **Figure 4B**, the  $T_g$  of Pebax 2533  
372 prior to microstructure re-arrangement was -76.35 °C. After the water treatment, the  $T_g$   
373 of the membrane was reduced to -78.65 °C (shown in **Table 2**), at the same time,  $T_m$   
374 was also found to decrease slightly, denoting a lower crystallinity degree, these results  
375 are in good agreement with the XRD results. The reduced crystallinity degree will result  
376 in increased chain segment mobility, and is favorable for gas permeability of Pebax  
377 2533 membranes.

378 **Table 2.**  $T_g$  and  $T_{m1}$  of PEO segments and  $T_{m2}$  of PA of Pebax 2533 membrane before and after

379 microstructure re-arrangement

Membrane	$T_g$ (°C)	$T_{m1}$ PEO (°C)	$T_{m2}$ PA (°C)
Pebax 2533	-76.35	11.36	100.76
Pebax 2533-3 h-25 °C	-78.65	10.56	100.56
Pebax 2533-24 h-25 °C	-78.45	10.46	100.86
Pebax 2533-72 h-25 °C	-78.26	10.06	100.56

380 The chemical structure of the Pebax 2533 membranes was characterized using FTIR  
381 (**Figure 4D**). The detailed peak assignments of Pebax 2533 are also listed in **Table 3**,  
382 which is consistent with data previously reported in the literature [53-55]. From the  
383 FTIR results, there was no new peak or peak shift in the Pebax 2533 membrane before  
384 and after water treatment, indicating no chemical interaction between the non-solvent  
385 water used in this study and Pebax 2533.

386 **Table 3.** FTIR peak assignments of Pebax 2533

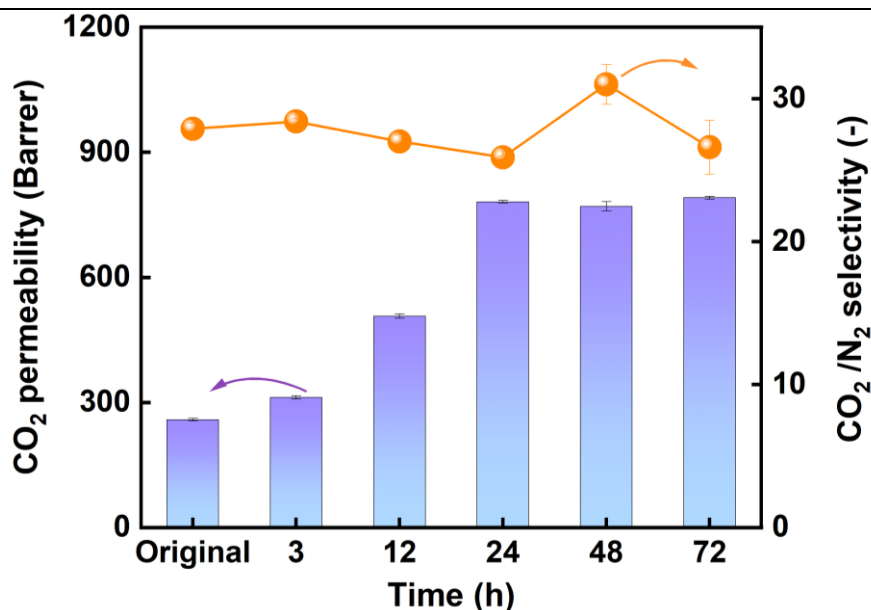
Wavenumber (cm <sup>-1</sup> )	Peak assignment	Ref
1106	stretching of -C-O-C-	[53]
1538	bending of N-H in PA	[53]
1638	stretching of -C=O in H-N-C=O	[54]
1734	stretching of -C=O in PA	[55]
2853	bending of -C-H	[55]

---

2923	bending of -C-H	[55]
3305	stretching of N-H in PA	[53]

---

387 Water uptake can also be an interesting parameter for Pebax 2533 membranes, as the  
388 presence of water vapor may have a significant impact on the CO<sub>2</sub> separation properties  
389 of Pebax membranes [56]. In the current study, it is found that Pebax 2533 membranes  
390 exhibited a slightly higher water uptake after the water treatment (from ~1.1% to ~1.4%,  
391 as shown in **Figure 4C**), but the overall water uptake remains in the low region.  
392 The CO<sub>2</sub>/N<sub>2</sub> separation performances of the Pebax 2533 treated with water for different  
393 duration time were also investigated, and results are presented in **Figure 5**. As indicated  
394 in the figure, the Pebax 2533 treated with water will always lead to a higher CO<sub>2</sub>  
395 permeability. As the water treatment duration time increased to 24 hours, a CO<sub>2</sub>  
396 permeability of 782.3 Barrer was documented, which is 3 times higher than the neat  
397 Pebax 2533 membrane (258.5 Barrer). In addition, the water-treated membrane  
398 presents a CO<sub>2</sub>/N<sub>2</sub> selectivity (25.9) comparable to the neat Pebax 2533 membranes  
399 (27.9). The underlying reason for this phenomenon can be that water treatment has  
400 resulted in an apparent loosening of chain segments previously partially ‘locked’ by  
401 dipole-dipole interactions, leading to the microstructure change and reduced  
402 crystallinity degree, and consequently a higher CO<sub>2</sub> permeability but little change in  
403 CO<sub>2</sub>/N<sub>2</sub> selectivity. Further increasing the water treatment time gains only slight  
404 improvement in CO<sub>2</sub> permeability; thus, 24 hours was selected as the water treatment  
405 duration in the further study.



406

407 **Figure. 5.** Gas separation performance of Pebax 2533 membranes with different water treatment

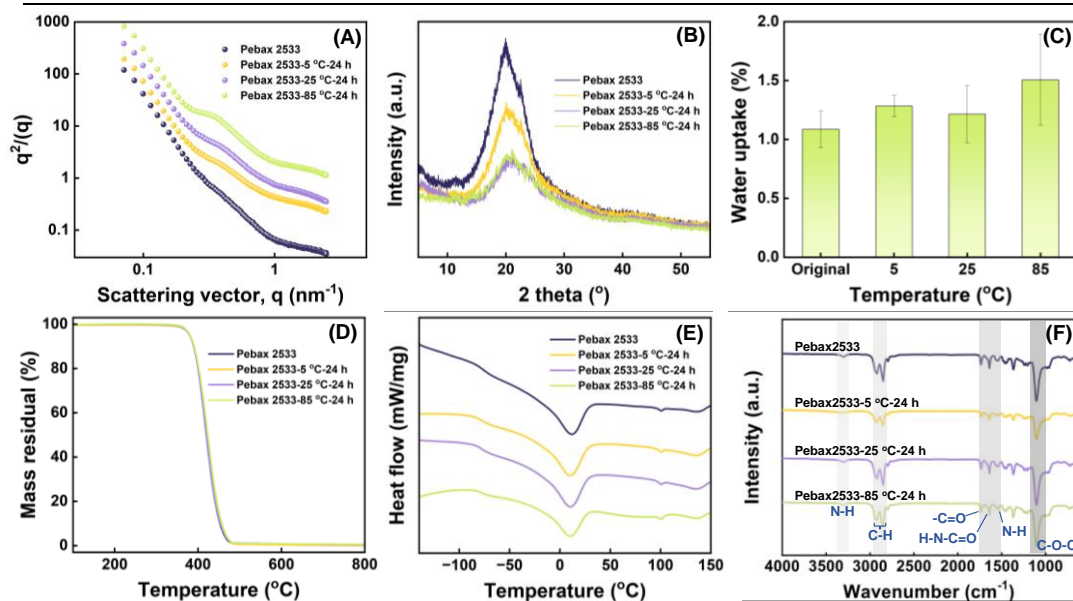
408 duration time, gas permeation test carried out with a feed pressure of 2 bar at 25 °C.

#### 409 **3.4 Effect of microstructure re-arrangement temperature**

410 It is well-known that membrane casting temperature also plays an important role in the  
411 membrane morphology and consequent gas separation properties [57, 58]. Therefore,  
412 in the current study, the water bath temperature was also changed to investigate its  
413 effect on the membrane's chemical-physical properties.

414 The Pebax membrane was treated with water at different temperatures (5 °C, 25 °C, 45  
415 °C, 65 °C, and 85 °C) for 24 hours, and the results are presented in **Figure 6**.

416



417

418

419

420

421

422

423

424

425

426

427

428

429

430

431

432

433

434

435

436

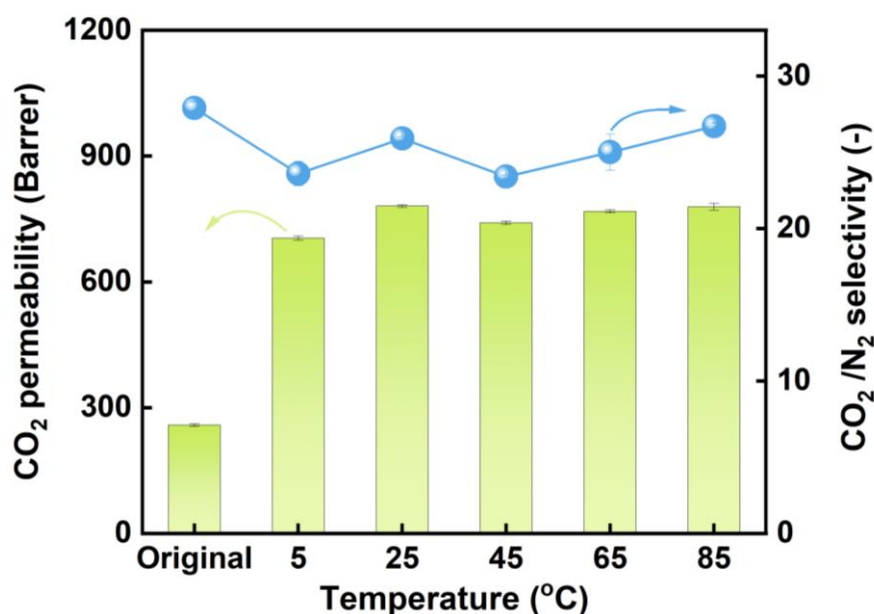
**Figure 6.** Chemical-physical characterization of Pebax 2533 before and after water-induced micro-phase separation. SAXS (A), XRD (B), water uptake (C), TGA (D), DSC (E), and FTIR (F) results of Pebax 2533 treated with water at different temperatures for 24 hours.

The SXAS data for the Pebax 2533 membrane obtained with different re-arrangement temperatures are similar to the results obtained from different duration times (**Figure 6A**). As the water treatment temperature increases, the wide first-order interference peak is observed at around  $q=0.4 \text{ nm}^{-1}$ , and it becomes more obverse as the water treatment temperature increases. In addition to the changes associated with peak-recognition ion clusters during treatment, another feature of **Figure 6A** is that the shape of the Pebax 2533 pre-peak scattering profile is quite different from that of the re-arrangement membranes. Although the exact physical significance of these scattered shapes is not fully known at present, it might be related to the differences in the spatial depiction of TEM images discussed in **Figure 3A**.

On the other hand, treating the Pebax 2533 membrane with high temperature also led to a lower crystallinity degree, as indicated by the XRD results shown in **Figure 6B**. In terms of the water uptake, the membrane treated with water at different temperatures presented similar trends compared to the different duration results, with only one exception ( $5 \text{ }^\circ\text{C}$ , shown in **Figure 6C**).

Considering the thermal properties, the membrane treated at different temperature

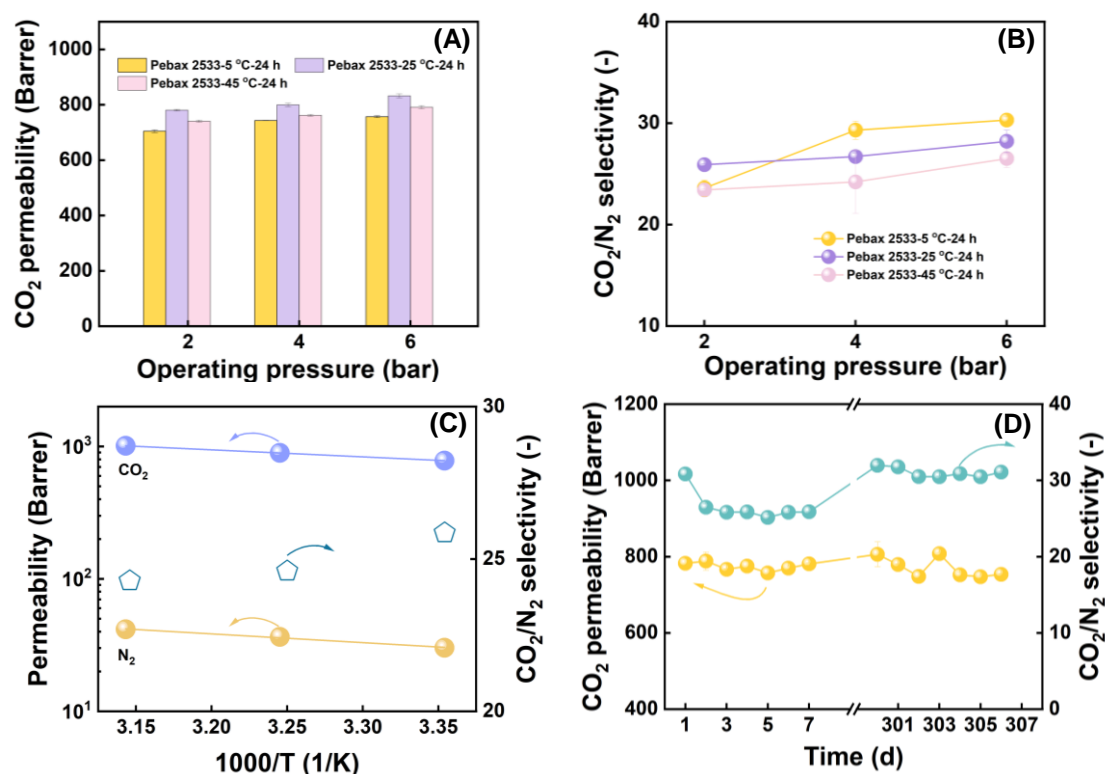
437 conditions also exhibited superior thermal stability precisely the same as the neat Pebax  
438 2533 (**Figure 6D**), while water treatment led to lower  $T_g$ ,  $T_m$ , and consequently lower  
439 crystallinity (**Figure 6E**), as confirmed by the XRD results. FTIR results also indicated  
440 that there is no chemical reaction between water and Pebax 2533 (**Figure 6F**), as there  
441 are no new peaks, and peak position shifting was observed.  
442 The above characterization indicates that the chemical composition and thermal  
443 stability of the Pebax 2533 membrane remained consistent before and after the  
444 microstructure re-arrangement. The CO<sub>2</sub> separation performances of the Pebax 2533  
445 membrane treated at different temperatures were tested and presented in **Figure 7**. It is  
446 clearly shown that the effect of re-arrangement temperature is minimal compared to the  
447 duration time, as almost all the re-arranged membranes exhibited a CO<sub>2</sub> permeability  
448 close to 800 Barrer and CO<sub>2</sub>/N<sub>2</sub> selectivity of ~25, regardless of the rearrangement  
449 temperature. Considering the energy cost and process convenience, the optimal  
450 rearrangement temperature is set as 25 °C.



451  
452 **Figure 7.** CO<sub>2</sub>/N<sub>2</sub> separation performance of Pebax 2533 membranes with different water treatment  
453 temperatures, gas permeation test carried out with a feed pressure of 2 bar at 25 °C. Pebax 2533  
454 membrane was treated with water for 24 hours

### 455 3.5 Gas permeation test conditions and long-term stability

456 Other than the membrane preparation parameters (e.g., water treatment temperature and  
457 soaking duration), it is well-accepted that operation parameters (e.g., testing  
458 temperature and feed pressure) also have an important influence on the membrane gas  
459 separation performances [59, 60]. Therefore, the effects of feed pressure and  
460 temperature were also explored. **Figure 8A** and **Figure 8B** show the CO<sub>2</sub> separation  
461 performance of water-treated Pebax 2533 with a feed pressure of 2, 4, and 6 bar. As  
462 can be seen from the figure, with the pressure increasing from 2 bar to 6 bar, the CO<sub>2</sub>  
463 permeability of the membrane material showed a slowly rising trend, as reported in the  
464 literature [61-63], while the CO<sub>2</sub>/N<sub>2</sub> selectivity remained stable, indicating the water-  
465 treated Pebax 2533 exhibited similar CO<sub>2</sub> separation behavior compared to the neat  
466 Pebax 2533 membrane.



467  
468 **Figure 8.** Effect of feed pressure on Pebax 2533 membrane CO<sub>2</sub> permeability (A) and selectivity  
469 (B); effect of feed temperature on Pebax 2533 membrane CO<sub>2</sub> permeability and selectivity (C).  
470 Long-term stability of Pebax 2533 membrane tested at a feed pressure of 2 bar at 25 °C (D). The



471    Pebax membranes were treated in water at 25 °C for 24 hours.

472                      In addition, the effect of test temperature was also investigated in the range of 25 °C to  
473                      45 °C. Generally, the increasing testing temperature will result in improved diffusivity  
474                      and reduced solubility, but the permeability (the product of diffusivity and solubility)  
475                      will typically increase.

476                      For Pebax 2533 membrane was treated in water at 25 °C for 24 hours, the relationship  
477                      between temperature and CO<sub>2</sub> gas permeability is shown in **Figure 8C**. As the operating  
478                      temperature increases from 25 °C to 45 °C, the CO<sub>2</sub> permeability of the membrane  
479                      material gradually increases from 782.3 Barrer to 1010.2 Barrer. It is well-accepted that  
480                      for a given polymer, the effect of temperature on gas permeability (*P*) in a temperature  
481                      range where there is no obvious thermal conversion can be described by the Arrhenius  
482                      equation [64]:

$$483 \quad P = P_0 \cdot \exp\left(-\frac{E_p}{RT}\right) \quad (4)$$

484                      Among them, *E<sub>p</sub>* and *P<sub>0</sub>* are called activation energy and pre-exponential factor,  
485                      respectively, which are two very important parameters in chemical kinetics. *R* is the  
486                      molar gas constant; *T* is the thermodynamic temperature. In the current study, the *E<sub>p</sub>*  
487                      values of CO<sub>2</sub> and N<sub>2</sub> were 10.2 and 12.6, respectively, with a correlation coefficient  
488                      (*R*<sup>2</sup>) always greater than 0.99

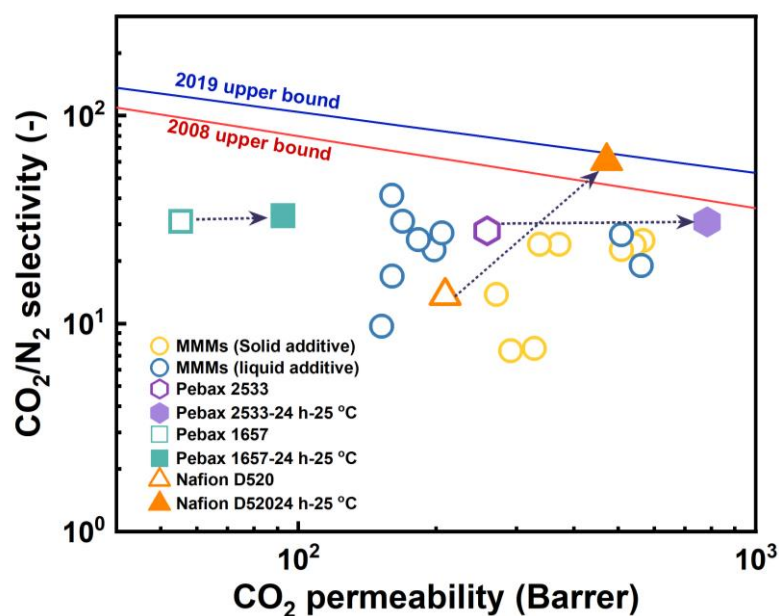
489                      Similar to many CO<sub>2</sub>-selective membrane materials, increasing testing temperature  
490                      results in higher CO<sub>2</sub> permeability but with lower CO<sub>2</sub>/N<sub>2</sub> selectivity [65]. In the current  
491                      study, increasing the testing temperature from 25 °C to 45 °C resulted in a negligible  
492                      reduction of CO<sub>2</sub>/N<sub>2</sub> selectivity, which is from 25.9 to 24.3, denoting its superior CO<sub>2</sub>  
493                      separation performances.

494                      Good long-term stability of membrane material is of critical importance in practical  
495                      applications. Therefore, the duration stability of the water-treated Pebax 2533  
496                      membranes were also tested for 7 days with a feed pressure of 2 bar at 25 °C. As shown  
497                      in **Figure 8D**, the CO<sub>2</sub> permeability and CO<sub>2</sub>/N<sub>2</sub> selectivity of the membrane is quite  
498                      stable during the 7 days continuous measurement process. In addition, the rearranged

499 membranes were stored in ambient conditions for about 10 months and it is found the  
500 membrane exhibited almost unchanged CO<sub>2</sub> separation performances, reflecting the  
501 excellent long-term stability of the re-arranged membranes, which shows great  
502 application potential in practical CO<sub>2</sub> separation applications.

### 503 3.6 Comparison of gas permeation results

504 The gas separation performances of the microstructure re-arrangement membranes  
505 prepared in this study were compared with literature values, as shown in **Table 6** and  
506 **Figure 9**. Notably, for Pebax 2533 membranes, after microstructure re-arrangement in  
507 DI water, the CO<sub>2</sub> permeability increased three-fold compared to the original membrane,  
508 while the CO<sub>2</sub>/N<sub>2</sub> selectivity remained unchanged. In contrast, the microstructure re-  
509 arrangement of Nafion membranes seems more effective in promoting CO<sub>2</sub>/N<sub>2</sub>  
510 permeability. The significantly improved performance in these membranes confirms  
511 that microstructure re-arrangement can be used as a technique to optimize CO<sub>2</sub>  
512 separation performance of block copolymer membranes, providing a new approach for  
513 the preparation of high-performance CO<sub>2</sub> capture membranes.



514

515 **Figure 9.** Robeson plot for the CO<sub>2</sub>/N<sub>2</sub> separation performance obtained from single-gas

516 permeation tests of Pebax 2533 membranes before and after microstructure re-arrangement.

517

Circles are literature data from Table 4

518

**Table 4.** Separation performance of Pebax membranes

Membrane	PCO <sub>2</sub> (Barrer)	$\alpha_{\text{CO}_2/\text{N}_2}$ (-)	Ref.
Pebax 2533+(20 wt.%) PEG 400	291.2	7.4	[55] (1)
Pebax 2533+(40 wt.%) PEG 400	327.8	7.6	[55] (1)
Pebax 2533+(0.02 wt.%) GO	371.4	24.0	[66] (2)
Pebax 2533+(0.1 wt.%) GO	336.8	24.0	[66] (2)
Pebax 2533+(20 wt.%)TPP	566.4	25.1	[67] (3)
Pebax 2533+(21 wt.%)TBT	542.5	23.9	[67] (3)
Pebax 2533+(22 wt.%)TCP	508.4	22.7	[67] (3)
Pebax 2533+(20 wt.%) [TMGH][Im]	271.1	13.8	[68] (4)
Pebax 2533+(15 wt.%) ZIF-8	508.4	22.7	[56] (5)
Pebax 2533+(10 wt.%) PS	152.1	9.7	[69] (6)
Pebax 2533+(10 wt.%) ZIF-Matrimid	160.3	16.9	[69] (6)
Pebax 2533+(3.4 wt.%) ZIF-7	198	22.6	[70] (7)
Pebax 2533+(3.4 wt.%) ZIF-7-NH <sub>2</sub>	206	27.3	[70] (7)
Pebax 2533+(3.4 wt.%) ZIF-7-CH <sub>3</sub> OH	562.0	19.0	[70] (7)
Pebax 2533+(0.5 wt.%) Apdems	183	25.3	[71] (8)
Pebax 2533+(1.0 wt.%) Apdems	169	31	[71] (8)
Pebax 2533+(2.0 wt.%) Apdems	160	41.3	[71] (8)
Pebax 2533	258.5	27.9	This work (9)
Pebax 2533-24 h-25 °C	782.3	30.8	This work (9)
Pebax 1657	55.3	31.0	This work (9)
Pebax 1657-24 h-25 °C	92.5	33.0	This work (9)
Nafion D520	209.3	13.6	This work (10)
Nafion D520-24 h-25 °C	472.0	60.6	This work (10)

519

(1) Single-gas permeation test conducted at dry state, with a feed pressure of 4 bar and 25 °C.

520

(2) Single-gas permeation test conducted at dry state, with a feed pressure of 1 bar and 35 °C.

521

(3) Single-gas permeation test conducted at dry state, with a feed pressure of 5 bar and 35 °C.

522

(4) Single-gas permeation test conducted at dry state, with a feed pressure of 4 bar and 25 °C.

523

(5) Single-gas permeation test conducted at dry state, with a feed pressure of 6 bar and 25 °C.

524

(6) Single-gas permeation test conducted at dry state, with a feed pressure of 1 bar and 35 °C.

525

(7) Single-gas permeation test conducted at dry state, with a feed pressure of 4.5 bar and 25 °C.

526 (8) Single-gas permeation test conducted at dry state, with a feed pressure of 10 bar and ambient  
527 temperature.

528 (9) Single-gas permeation test conducted at dry state, with a feed pressure of 2 bar and 25 °C.

529 (10) Mixed-gas permeation test conducted at 100% RH, with a feed pressure of 2 bar and ambient  
530 temperature.

#### 531 **4. Conclusions**

532 In the current work, a non-solvent induced microstructure re-arrangement process was  
533 applied to improve the CO<sub>2</sub> separation performances of block copolymer-based  
534 membranes. Different non-solvents were employed to trigger the microstructure  
535 transition, among which the DI water performs the best in terms of CO<sub>2</sub> separation  
536 performances. The obtained membranes were thoroughly characterized, confirming  
537 that the DI water treatment results in more tightly connected ionic microdomains and  
538 lower crystallinity degrees of the re-arranged membrane matrix, which are the  
539 underlying reasons for the improved CO<sub>2</sub> separation performances. Experiments  
540 indicate that the DI water-induced microstructure arrangement is a physical process that  
541 does not influence the thermal stability and chemical stability of the Pebax 2533  
542 membranes. The gas permeation test results reveal that the CO<sub>2</sub> permeability of the  
543 Pebax 2533 was greatly improved (from 258.5 Barrer to 782.3 Barrer), while the  
544 CO<sub>2</sub>/N<sub>2</sub> selectivity is almost unchanged. Furthermore, the Pebax 2533 membranes also  
545 exhibited promising long-term stability after 300 days storage, denoting its great  
546 potential in CO<sub>2</sub> separation applications.

547 Future work can be carried out to explore the separation performance of the membranes  
548 under humid conditions. Developing thin-film-composite membranes using  
549 microstructure rearranged membranes can be another option worth trying.

550 **Acknowledgements**

551 This work acknowledges the financial support from Sichuan Science and Technology  
552 Program (2021YFH0116) and National Natural Science Foundation of China (No.  
553 52170112) and DongFang Boiler Co.,Ltd.(3522015).

554 **References**

- 555 [1] M. Kárászová, B. Zach, Z. Petrusová, V. Červenka, M. Bobák, M. Šyc, P. Izák,  
556 Post-combustion carbon capture by membrane separation, Review, Separation and  
557 Purification Technology, 238 (2020) 116448.
- 558 [2] R. Krishna, J.M. van Baten, A comparison of the CO<sub>2</sub> capture characteristics of  
559 zeolites and metal–organic frameworks, Separation and Purification Technology, 87  
560 (2012) 120-126.
- 561 [3] H. Rasouli, K. Nguyen, M.C. Iliuta, Recent advancements in carbonic anhydrase  
562 immobilization and its implementation in CO<sub>2</sub> capture technologies: A review,  
563 Separation and Purification Technology, 296 (2022) 121299.
- 564 [4] M. Shen, L. Tong, S. Yin, C. Liu, L. Wang, W. Feng, Y. Ding, Cryogenic  
565 technology progress for CO<sub>2</sub> capture under carbon neutrality goals: A review,  
566 Separation and Purification Technology, 299 (2022) 121734.
- 567 [5] A. Car, C. Stropnik, W. Yave, K.-V. Peinemann, Pebax®/polyethylene glycol blend  
568 thin film composite membranes for CO<sub>2</sub> separation: Performance with mixed gases,  
569 Separation and Purification Technology, 62 (2008) 110-117.
- 570 [6] S. Atchariyawut, R. Jiratananon, R. Wang, Mass transfer study and modeling of  
571 gas–liquid membrane contacting process by multistage cascade model for CO<sub>2</sub>  
572 absorption, Separation and Purification Technology, 63 (2008) 15-22.
- 573 [7] A. Bos, I.G.M. Pünt, M. Wessling, H. Strathmann, Plasticization-resistant glassy  
574 polyimide membranes for CO<sub>2</sub>/CO<sub>4</sub> separations, Separation and Purification  
575 Technology, 14 (1998) 27-39.
- 576 [8] M. Vinoba, M. Bhagiyalakshmi, Y. Alqaheem, A.A. Alomair, A. Pérez, M.S. Rana,  
577 Recent progress of fillers in mixed matrix membranes for CO<sub>2</sub> separation: A review,  
578 Separation and Purification Technology, 188 (2017) 431-450.
- 579 [9] T.A. Centeno, A.B. Fuertes, Carbon molecular sieve membranes derived from a  
580 phenolic resin supported on porous ceramic tubes, Separation and Purification  
581 Technology, 25 (2001) 379-384.
- 582 [10] E. Adatoz, A.K. Avci, S. Keskin, Opportunities and challenges of MOF-based  
583 membranes in gas separations, Separation and Purification Technology, 152 (2015)  
584 207-237.
- 585 [11] N. Liu, J. Cheng, W. Hou, C. Yang, X. Yang, J. Zhou, Bottom-up synthesis of two-  
586 dimensional composite via CuBDC-n<sub>s</sub> growth on multilayered MoS<sub>2</sub> to boost CO<sub>2</sub>

- 587 permeability and selectivity in Pebax-based mixed matrix membranes, Separation and  
588 Purification Technology, 282 (2022) 120007.
- 589 [12] S. Wang, X. Li, H. Wu, Z. Tian, Q. Xin, G. He, D. Peng, S. Chen, Y. Yin, Z.J.E.  
590 Jiang, E. Science, Advances in high permeability polymer-based membrane materials  
591 for CO<sub>2</sub> separations, Energy Environmental Science, 9 (2016) 1863-1890.
- 592 [13] M.M. Dal-Cin, A. Kumar, L.J. Layton, Revisiting the experimental and theoretical  
593 upper bounds of light pure gas selectivity–permeability for polymeric membranes,  
594 Journal of Membrane Science, 323 (2008) 299-308.
- 595 [14] S.R. Reijerkerk, A. Arun, R.J. Gaymans, K. Nijmeijer, M.J. Wessling, Tuning of  
596 mass transport properties of multi-block copolymers for CO<sub>2</sub> capture applications,  
597 Journal of Membrane Science, 359 (2010) 54-63.
- 598 [15] M. Buonomenna, W. Yave, G.J. Golemme, Some approaches for high performance  
599 polymer based membranes for gas separation: block copolymers, carbon molecular  
600 sieves and mixed matrix membranes, RSC advances, 2 (2012) 10745-10773.
- 601 [16] H.J. Min, Y.J. Kim, M. Kang, C.-H. Seo, J.-H. Kim, J.H. Kim, Crystalline  
602 elastomeric block copolymer/ionic liquid membranes with enhanced mechanical  
603 strength and gas separation properties, Journal of Membrane Science, 660 (2022)  
604 120837.
- 605 [17] T. Rajasekhar, M. Trinadh, P. Veera Babu, A.V.S. Sainath, A.V.R. Reddy, Oil–  
606 water emulsion separation using ultrafiltration membranes based on novel blends of  
607 poly(vinylidene fluoride) and amphiphilic tri-block copolymer containing carboxylic  
608 acid functional group, Journal of Membrane Science, 481 (2015) 82-93.
- 609 [18] H. Mizuno, K. Hashimoto, R. Tamate, H. Kokubo, K. Ueno, X. Li, M. Watanabe,  
610 Microphase-separated structures of ion gels consisting of ABA-type block copolymers  
611 and an ionic liquid: A key to escape from the trade-off between mechanical and  
612 transport properties, Polymer, 206 (2020) 122849.
- 613 [19] Z. Dai, J. Deng, H. Aboukeila, J. Yan, L. Ansaloni, K.P. Mineart, M. Giacinti  
614 Baschetti, R.J. Spontak, L. Deng, Highly CO<sub>2</sub>-permeable membranes derived from a  
615 midblock-sulfonated multiblock polymer after submersion in water, NPG Asia  
616 Materials, 11 (2019) 1-7.
- 617 [20] Z. Dai, H. Aboukeila, L. Ansaloni, J. Deng, M.G. Baschetti, L.J. Deng,  
618 Nafion/PEG hybrid membrane for CO<sub>2</sub> separation: Effect of PEG on membrane micro-  
619 structure and performance, Separation Purification Technology, 214 (2019) 67-77.
- 620 [21] S. Bandehali, A. Moghadassi, F. Parvizian, S.M. Hosseini, T. Matsuura,  
621 E.J.J.o.E.C. Joudaki, Advances in high carbon dioxide separation performance of poly  
622 (ethylene oxide)-based membranes, Journal of Energy Chemistry, 46 (2020) 30-52.
- 623 [22] W.-S. Sun, M.-J. Yin, W.-H. Zhang, S. Li, N. Wang, Q.-F.J.A. An, Green  
624 techniques for rapid fabrication of unprecedentedly high-performance PEO membranes  
625 for CO<sub>2</sub> capture, Sustainable Chemistry Engineering, 9 (2021) 10167-10175.
- 626 [23] A.S. Embaye, L. Martínez-Izquierdo, M. Malankowska, C. Téllez, J.J. Coronas,  
627 Poly (ether-block-amide) copolymer membranes in CO<sub>2</sub> separation applications,  
628 Energy Fuels, 35 (2021) 17085-17102.



- 629 [24] M. Isanejad, N. Azizi, T.J. Mohammadi, Pebax membrane for CO<sub>2</sub>/CH<sub>4</sub> separation:  
630 Effects of various solvents on morphology and performance, *Journal of Applied*  
631 *Polymer Science*, 134 (2017).
- 632 [25] S. Ahmad, S. Lian, Y. Tan, R. Li, Q. Zhao, C. Song, Q. Liu, S.J. Lu, Solvent  
633 influence on the textural properties and CO<sub>2</sub>/N<sub>2</sub> separation performance of novel Pebax-  
634 1657/attapulgite mixed matrix membranes, *Journal of Environmental Chemical*  
635 *Engineering*, 9 (2021) 105806.
- 636 [26] Y.J. Wang, Nondestructive creation of ordered nanopores by selective swelling of  
637 block copolymers: toward homoporous membranes, *Accounts of chemical research*, 49  
638 (2016) 1401-1408.
- 639 [27] Z. Wang, R. Liu, H. Yang, Y.J. Wang, Nanoporous polysulfones with in situ  
640 PEGylated surfaces by a simple swelling strategy using paired solvents, *Chemical*  
641 *Communications*, 53 (2017) 9105-9108.
- 642 [28] Z. Wang, X. Yao, Y.J. Wang, Swelling-induced mesoporous block copolymer  
643 membranes with intrinsically active surfaces for size-selective separation, *Journal of*  
644 *Materials Chemistry A*, 22 (2012) 20542-20548.
- 645 [29] D. Pye, H. Hoehn, M.J. Panar, Measurement of gas permeability of polymers. I.  
646 Permeabilities in constant volume/variable pressure apparatus, *Journal of Applied*  
647 *Polymer Science*, 20 (1976) 1921-1931.
- 648 [30] K. Jirsakova, P. Stanovský, P. Dytrych, L. Moravkova, K. Příbylová, Z. Petrusova,  
649 J.C. Jansen, P.J. Izak, Organic vapour permeation in amorphous and semi-crystalline  
650 rubbery membranes: Experimental data versus prediction by solubility parameters,  
651 *Journal of Membrane Science*, 627 (2021) 119211.
- 652 [31] R. Su, G. Liu, H. Sun, Z.J. Yong, A new method to measure the three-dimensional  
653 solubility parameters of acrylate rubber and predict its oil resistance, *Polymer Bulletin*,  
654 (2022) 1-14.
- 655 [32] X. Ren, J. Ren, H. Li, S. Feng, M.J. Deng, Poly (amide-6-b-ethylene oxide)  
656 multilayer composite membrane for carbon dioxide separation, *International Journal of*  
657 *Greenhouse Gas Control*, 8 (2012) 111-120.
- 658 [33] J. Durkee, *Cleaning with solvents: science and technology*, William Andrew, 2013.
- 659 [34] V. Pirouzfard, N. Roustaie, M. Salimi, C.-H. Su, Gas Transport Characteristics of  
660 Mixed Matrix Membrane Containing MIL-100 (Fe) Metal-Organic Frameworks and  
661 PEBAX Precursors, (2021).
- 662 [35] A.P. Isfahani, B. Ghalei, K. Wakimoto, R. Bagheri, E. Sivaniah, M.J. Sadeghi,  
663 Plasticization resistant crosslinked polyurethane gas separation membranes, *Journal of*  
664 *Materials Chemistry A*, 4 (2016) 17431-17439.
- 665 [36] M.S. Maleh, A.J. Raisi, In-situ growth of ZIF-8 nanoparticles in Pebax-2533 for  
666 facile preparation of high CO<sub>2</sub>-selective mixed matrix membranes, *Colloids Surfaces*  
667 *A: Physicochemical Engineering Aspects*, 659 (2023) 130747.
- 668 [37] V. Nafisi, M.-B.J. Hägg, Interfaces, Development of nanocomposite membranes  
669 containing modified Si nanoparticles in PEBAX-2533 as a block copolymer and 6FDA-  
670 durene diamine as a glassy polymer, *ACS Applied Materials*, 6 (2014) 15643-15652.

- 671 [38] M.S. Maleh, A.J. Raisi, Preparation of high performance mixed matrix membranes  
672 by one-pot synthesis of ZIF-8 nanoparticles into Pebax-2533 for CO<sub>2</sub> separation,  
673 Chemical Engineering Research Design, 186 (2022) 266-275.
- 674 [39] Y. Wu, D. Zhao, S. Chen, J. Ren, K. Hua, H. Li, M. Deng, The effect of structure  
675 change from polymeric membrane to gel membrane on CO<sub>2</sub> separation performance,  
676 Separation and Purification Technology, 261 (2021) 118243.
- 677 [40] N. Azizi, M.R. Hojjati, M.M.J.S. Zarei, Study of CO<sub>2</sub> and CH<sub>4</sub> permeation  
678 properties through prepared and characterized blended Pebax-2533/PEG-200  
679 membranes, Silicon, 10 (2018) 1461-1467.
- 680 [41] P. Bernardo, J.C. Jansen, F. Bazzarelli, F. Tasselli, A. Fuoco, K. Friess, P. Izák, V.  
681 Jarmarová, M. Kačírková, G. Clarizia, Gas transport properties of Pebax®/room  
682 temperature ionic liquid gel membranes, Separation and Purification Technology, 97  
683 (2012) 73-82.
- 684 [42] S.-Y. Kim, J.-S. Kim, J.H. Lee, J.H. Kim, T.-S. Han, Comparison of microstructure  
685 characterization methods by two-point correlation functions and reconstruction of 3D  
686 microstructures using 2D TEM images with high degree of phase clustering, Materials  
687 Characterization, 172 (2021) 110876.
- 688 [43] J.P. Sheth, J. Xu, G.L.J. Wilkes, Solid state structure–property behavior of  
689 semicrystalline poly (ether-block-amide) PEBA<sup>®</sup> thermoplastic elastomers, Polymer,  
690 44 (2003) 743-756.
- 691 [44] Z. Dai, L. Ansaloni, J.J. Ryan, R.J. Spontak, L. Deng, Incorporation of an ionic  
692 liquid into a midblock-sulfonated multiblock polymer for CO<sub>2</sub> capture, Journal of  
693 Membrane Science, 588 (2019) 117193.
- 694 [45] Z. Dai, L. Ansaloni, J.J. Ryan, R.J. Spontak, L.J.G.C. Deng, Nafion/IL hybrid  
695 membranes with tuned nanostructure for enhanced CO<sub>2</sub> separation: Effects of ionic  
696 liquid and water vapor, Green Chemistry  
697 20 (2018) 1391-1404.
- 698 [46] V. Hartmann, T. Kothe, S. Pöller, E. El-Mohsnawy, M.M. Nowaczyk, N. Plumeré,  
699 W. Schuhmann, M.J.P.C.C.P. Rögner, Redox hydrogels with adjusted redox potential  
700 for improved efficiency in Z-scheme inspired biophotovoltaic cells, Physical Chemistry  
701 Chemical Physics  
702 16 (2014) 11936-11941.
- 703 [47] T. Zhu, X. Yang, Y. Zheng, X. He, F. Chen, J.J. Luo, Preparation of poly (ether -  
704 block - amide)/poly (amide - co - poly (propylene glycol)) random copolymer blend  
705 membranes for CO<sub>2</sub>/N<sub>2</sub> separation, Polymer Engineering Science, 59 (2019) E14-E23.
- 706 [48] N. Azizi, M.R. Hojjati, M.M.J. Zarei, Study of CO<sub>2</sub> and CH<sub>4</sub> permeation properties  
707 through prepared and characterized blended Pebax-2533/PEG-200 membranes, Silicon,  
708 10 (2018) 1461-1467.
- 709 [49] S. Kalantari, M. Omidkhah, A.E. Amooghin, T.J. Matsuura, Superior interfacial  
710 design in ternary mixed matrix membranes to enhance the CO<sub>2</sub> separation performance,  
711 Applied Materials Today, 18 (2020) 100491.
- 712 [50] H. Zhao, Q. Xie, X. Ding, R. Cai, X. Tan, Y.J.S. Zhang, Advanced mixed matrix



- 713 membranes of Pebax embedded with amino acid ionic liquids@ PIM core-shell  
714 composite nanoparticles for CO<sub>2</sub> separation, Separation and Purification Technology,  
715 263 (2021) 118350.
- 716 [51] P. Bernardo, J.C. Jansen, F. Bazzarelli, F. Tasselli, A. Fuoco, K. Friess, P. Izák, V.  
717 Jarmarová, M. Kačírková, G.J. Clarizia, Gas transport properties of Pebax®/room  
718 temperature ionic liquid gel membranes, Separation Purification Technology, 97 (2012)  
719 73-82.
- 720 [52] M.M. Rahman, V. Filiz, S. Shishatskiy, C. Abetz, S. Neumann, S. Bolmer, M.M.  
721 Khan, V.J. Abetz, PEBA<sup>X</sup>® with PEG functionalized POSS as nanocomposite  
722 membranes for CO<sub>2</sub> separation, Journal of Membrane Science, 437 (2013) 286-297.
- 723 [53] H. Sanaeepur, S. Mashhadikhan, G. Mardassi, A. Ebadi Amooghin, B. Van der  
724 Bruggen, A.J.K.J.o.C.E. Moghadassi, Aminosilane cross-linked poly ether-block-  
725 amide PEBA<sup>X</sup> 2533: Characterization and CO<sub>2</sub> separation properties, Korean Journal  
726 of Chemical Engineering, 36 (2019) 1339-1349.
- 727 [54] N.L. Le, Y. Wang, T.-S.J. Chung, Pebax/POSS mixed matrix membranes for  
728 ethanol recovery from aqueous solutions via pervaporation, Journal of Membrane  
729 Science, 379 (2011) 174-183.
- 730 [55] N. Azizi, H.R. Mahdavi, M. Isanejad, T.J. Mohammadi, Effects of low and high  
731 molecular mass PEG incorporation into different types of poly (ether-b-amide)  
732 copolymers on the permeation properties of CO<sub>2</sub> and CH<sub>4</sub>, Journal of Polymer Research,  
733 24 (2017) 1-14.
- 734 [56] V. Nafisi, M.-B.J. Hägg, Development of dual layer of ZIF-8/PEBA<sup>X</sup>-2533 mixed  
735 matrix membrane for CO<sub>2</sub> capture, Journal of Membrane Science, 459 (2014) 244-255.
- 736 [57] S. Li, S.-M. Chang, M.-J. Yin, W.-H. Zhang, W.-S. Sun, A. Shiue, Q.-F.J. An,  
737 Build up 'highway' in membrane via solvothermal annealing for high-efficient CO<sub>2</sub>  
738 capture, Journal of Membrane Science, 652 (2022) 120444.
- 739 [58] E. Lasseguette, L. Fielder-Dunton, Q. Jian, M.-C.J. Ferrari, The Effect of Solution  
740 Casting Temperature and Ultrasound Treatment on PEBA<sup>X</sup> MH-1657/ZIF-8 Mixed  
741 Matrix Membranes Morphology and Performance, Membranes, 12 (2022) 584.
- 742 [59] Z. Dai, L. Ansaloni, J.J. Ryan, R.J. Spontak, L.J. Deng, Nafion/IL hybrid  
743 membranes with tuned nanostructure for enhanced CO<sub>2</sub> separation: Effects of ionic  
744 liquid and water vapor, Green Chemistry, 20 (2018) 1391-1404.
- 745 [60] S. Haider, A. Lindbråthen, J.A. Lie, I.C.T. Andersen, M.-B.J. Hägg, CO<sub>2</sub>  
746 separation with carbon membranes in high pressure and elevated temperature  
747 applications, Separation Purification Technology, 190 (2018) 177-189.
- 748 [61] E. Ahmadpour, A.A. Shamsabadi, R.M. Behbahani, M. Aghajani, A.J. Kargari,  
749 Study of CO<sub>2</sub> separation with PVC/Pebax composite membrane, Journal of Natural Gas  
750 Science Engineering, 21 (2014) 518-523.
- 751 [62] F. Dorosti, M. Omidkhah, R.J. Abedini, Design, Fabrication and characterization  
752 of Matrimid/MIL-53 mixed matrix membrane for CO<sub>2</sub>/CH<sub>4</sub> separation, Chemical  
753 Engineering Research, 92 (2014) 2439-2448.
- 754 [63] S.R. Reijerkerk, M.H. Knoef, K. Nijmeijer, M.J. Wessling, Poly (ethylene glycol)

- 755 and poly (dimethyl siloxane): Combining their advantages into efficient CO<sub>2</sub> gas  
756 separation membranes, *Journal of membrane science*, 352 (2010) 126-135.
- 757 [64] L. Liu, W. Chen, Y. Li, An overview of the proton conductivity of nafion  
758 membranes through a statistical analysis, *Journal of Membrane Science*, 504 (2016) 1-  
759 9.
- 760 [65] Z. Zhang, S. Rao, Y. Han, R. Pang, W.S.W. Ho, CO<sub>2</sub>-selective membranes  
761 containing amino acid salts for CO<sub>2</sub>/N<sub>2</sub> separation, *Journal of Membrane Science*, 638  
762 (2021) 119696.
- 763 [66] R. Casadei, M. Giacinti Baschetti, M.J. Yoo, H.B. Park, L.J. Giorgini, Pebax®  
764 2533/graphene oxide nanocomposite membranes for carbon capture, *Membranes*, 10  
765 (2020) 188.
- 766 [67] Y. Wu, D. Zhao, J. Ren, Y. Qiu, Y. Feng, M.J. Deng, Effect of triglyceride on the  
767 microstructure and gas permeation performance of Pebax-based blend membranes,  
768 *Separation Purification Technology*, 256 (2021) 117824.
- 769 [68] H. Jiang, L. Bai, B. Yang, S. Zeng, H. Dong, X.J. Zhang, The effect of protic ionic  
770 liquids incorporation on CO<sub>2</sub> separation performance of Pebax-based membranes,  
771 *Chinese Journal of Chemical Engineering*, 43 (2022) 169-176.
- 772 [69] A. Ansari, A.H. Navarchian, H.J. Rajati, Permselectivity improvement of  
773 PEBAX® 2533 membrane by addition of glassy polymers (Matrimid® and polystyrene)  
774 for CO<sub>2</sub>/N<sub>2</sub> separation, *Journal of Applied Polymer Science*, 139 (2022) 51556.
- 775 [70] J. Gao, H. Mao, H. Jin, C. Chen, A. Feldhoff, Y.J. Li, Functionalized ZIF-  
776 7/Pebax® 2533 mixed matrix membranes for CO<sub>2</sub>/N<sub>2</sub> separation, *Microporous*  
777 *Mesoporous Materials*, 297 (2020) 110030.
- 778 [71] H. Sanaeepur, S. Mashhadikhan, G. Mardassi, A. Ebadi Amooghin, B. Van der  
779 Bruggen, A.J. Moghadassi, Aminosilane cross-linked poly ether-block-amide PEBAX  
780 2533: Characterization and CO<sub>2</sub> separation properties, *Korean Journal of Chemical*  
781 *Engineering*, 36 (2019) 1339-1349.
- 782